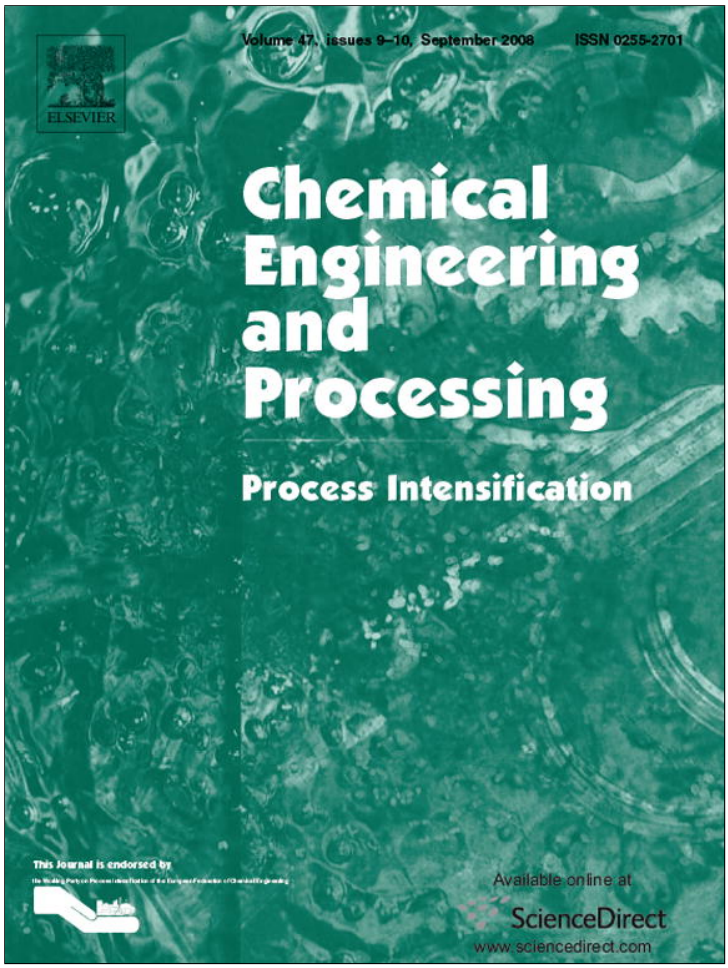

Available online at www.sciencedirect.com
ScienceDirect
Chemical Engineering and Processing 47 (2008) 1666–1677
Chemical Engineering and Processing Process Intensification
www.elsevier.com/locate/cep

Modelling agglomeration degree in sucrose crystallisation

N. Faria [a], S. Feyo de Azevedo [a,*], F.A. Rocha [a], M.N. Pons [b]

[a] *Departamento de Engenharia Qímica, Faculdade de Engenharia, Universidade do Porto, Rua Dr. Roberto Frias, 4200-465 Porto, Portugal*
[b] *Laboratoire des Sciences du Génie Chimique, CNRS-ENSIC-INPL, 1 rue Grandville, BP 451, F-54001 Nancy Cedex, France*

Received 1 May 2007; received in revised form 31 August 2007; accepted 14 September 2007
Available online 20 September 2007

Abstract

A model to simulate the time evolution of the distribution of agglomeration degree of sucrose crystals is deduced and validated against experimental data obtained through an image analysis technique. The crystallisation laboratory facility, procedures and the resulting experimental data are described. The model employed includes nucleation, growth, growth rate dispersion and agglomeration kinetics. The experimental data consists of on-line temperature and sugar content profiles in addition to off-line image analysis measurements of crystal size and agglomeration degree. Good agreement is obtained between the experimental and simulated results. This new model represents a most relevant tool for acquiring new knowledge of crystallisation/agglomeration mechanisms.

PACS: 81.10.Aj; 81.10.−h

Keywords: Crystal morphology; Agglomeration; Agglomeration degree; Sucrose

1. Introduction

Crystallisation is both a widely used and one of the least understood industrial unit operations.

There are several properties which influence the behaviour of crystallising systems. Some properties like temperature and the properties of the solution, such as solute concentration, or ionic strength, are usually relatively easy to measure and quantify. Difficulties appear when properties of solids must be taken into account.

The discrete nature of the solid contents and the huge number of particles present in industrial crystallisation processes make it impossible to quantify the properties of each particle and the interactions between each particle and the liquid phase. This problem has been addressed through statistical methods which allow the characterisation of large numbers of particles by a relatively small group of parameters.

From the properties of crystals, size is undoubtly most significant, not only for the properties of the final product but also to their behaviour during the crystallisation process. It is not surprising that the crystal size distribution has typically been the only crystal property taken into account in industrial crystallisation studies.

Other properties such as crystal morphology should be relevant to the behaviour of the crystal populations, either during the crystallisation process or as a final product. On one hand, some research [1–7] clearly points in that direction. On the other hand, there has been very little work addressing the problem of quantifying such properties in large populations.

This work is part of an ongoing effort to quantify the morphology of crystal populations and use this information in the prediction of their properties and behaviour. It is based on an image analysis technique which allows the quantification of crystal morphology [8]. Through this technique it was possible for the first time to quantify the agglomeration degree of crystals as a bounded parameter. Through an image analysis algorithm and an operator trained statistical method, each crystal is classified, according to its apparent complexity, with an agglomeration degree between 0 and 1 (simple crystal and very agglomerated crystal, respectively). Figs. 1 and 2 illustrate scanning electron microscopy images of a simple and a little agglomerated sucrose crystals, respectively. In the present work a crystallisation model for predicting this new parameter is deduced and validated.

* Corresponding author. Tel.: +351 225081694; fax: +351 225081632.
E-mail address: sfeyo@fe.up.pt (S.F. de Azevedo).

0255-2701/$ – see front matter © 2007 Elsevier B.V. All rights reserved.
doi:10.1016/j.cep.2007.09.008

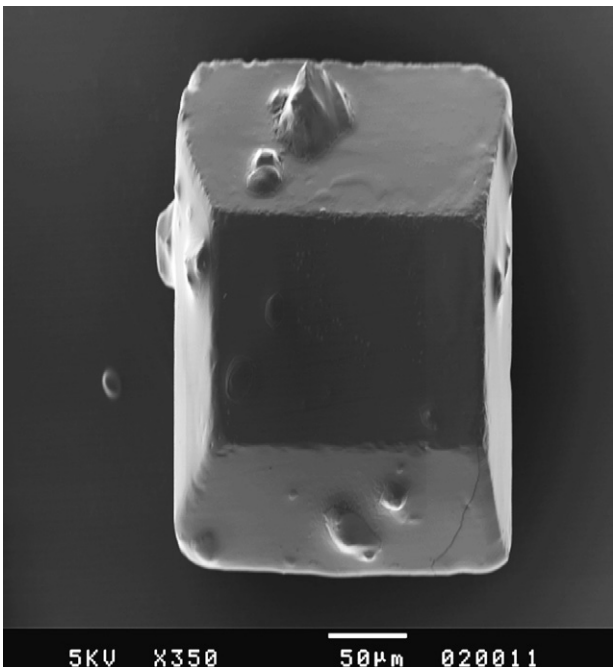

Fig. 1. SEM micrograph of a crystal classified as simple.

Firstly, the experimental set-up used to produce the sugar crystal populations is described. Most relevant for the success of this work are the design of the crystalliser – including the stirrer – and the operational smoothness of the temperature conditioning control system.

The model itself is based on a discretisation of the population balance equation (1) [9] presented for the first time by Hounslow et al. [10]. It was further developed by Chorão and Feyo de Azevedo [11] for the simulation of an industrial semi-bath crystalliser. The main differences between the present model and the previous one concern the adaptation to a laboratory crystallisation unit, namely the growth kinetics equation, and the simulation, for the first time, of the agglomeration degree of crystals.

$$\frac{\partial N}{\partial t} + \frac{\partial (GN)}{\partial L} - D_g \frac{\partial^2 N}{\partial L^2} = B - D \quad (1)$$

The main challenge addressed by the work of Chorão, Hounslow and others has been to take into account the effects of nucleation, agglomeration, crystal growth and growth rate dispersion in the simulation of the crystal size distribution (CSD) during a crystallisation process. Model validation was based only on measurements of the CSD and the evolution of the solids concentration. One problem is that the CSD is a product of three phenomena (growth, nucleation and agglomeration) simultaneously. The distinction among the effect of each one depends on the model being employed, compromising the model validation. In the present work, a model is deduced to simulate the evolution of the agglomeration degree, measured by an image analysis technique previously developed by the authors [8]. This new variable and the corresponding experimental data are then used in parameter estimation and validation of the entire model. This way, a direct measurement of agglomeration is introduced. As the agglomeration kinetics may now be accounted for by an independent measure, its effect on the evolution of the CSD may now be well established, allowing for a sustained quantification of the three crystallisation phenomena.

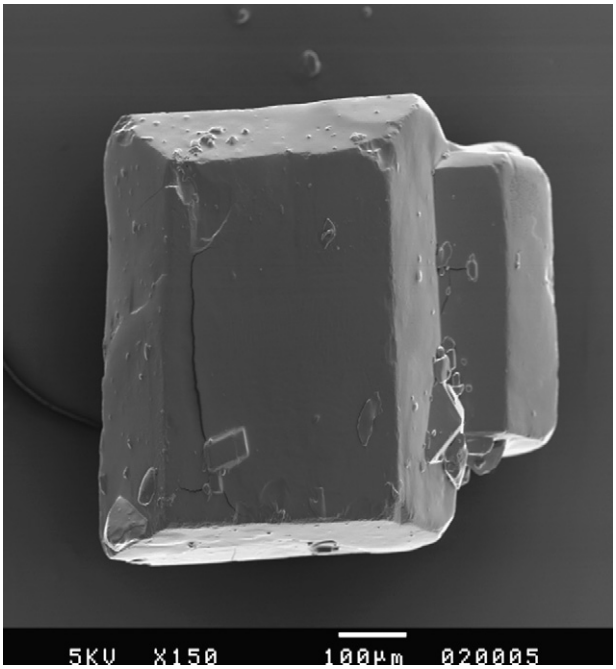

Fig. 2. SEM micrograph of a crystal classified as little agglomerated.

2. Experimental set-up

The experimental set-up employed in this work is based on a 2 L batch crystalliser made of acrylic, presented in the schematic shown in Fig. 3. The temperature inside the crystalliser is conditioned by making water circulate in the jacket that surrounds the crystallising chamber.

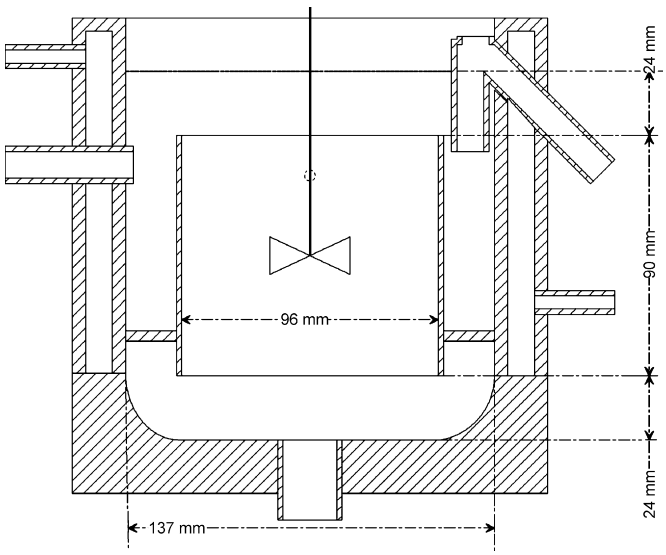

Fig. 3. Design schematic of the crystalliser.

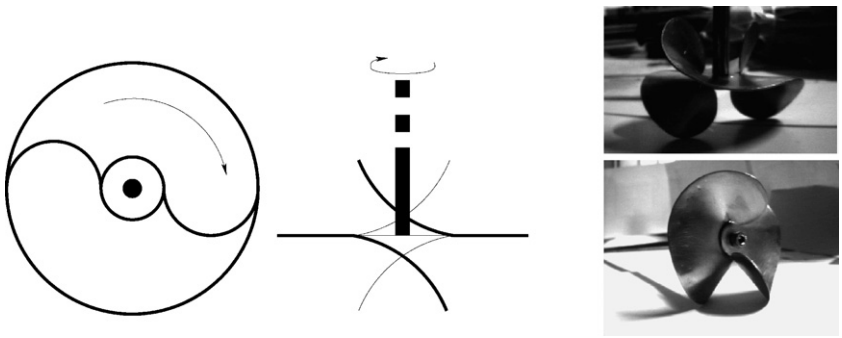

Fig. 4. The stirrer: drawings and photographs.

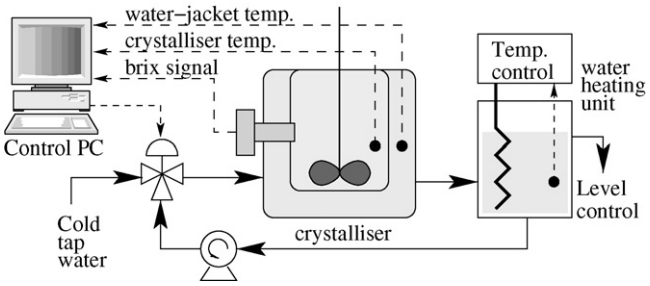

Fig. 5. The temperature conditioning set-up.

The geometry of the crystallising chamber was projected to avoid the formation of crystal incrustations in less agitated zones. A good level of mixing was achieved by the introduction of a draft tube and the use of a stirrer specially designed for this set-up. Additional schematics and photographs of the stirrer are presented in Fig. 4. The stirrer was designed to avoid crystal breakage while maintaining a good level of mixing.

2.1. Temperature conditioning and data acquisition

The temperature in the crystalliser is regulated by hot/cold water circulation in a water jacket. Fig. 5 illustrates this design. The temperature in the crystalliser is measured by two PT100 sensors at two different positions inside the crystalliser. The jacket temperature is measured by a thermocouple positioned at the water inlet. All measurements are collected every 10 s using a PC equipped with A/D D/A data acquisition card. The sucrose concentration, measured as the mass percentage of sucrose in solution (degree brix, $^{\circ}Bx$), is measured in real time by an on-line process refractometer (Schmidt & Hensch IPR2). The signal is sent via RS-232 to the PC.

With the values of the temperature and degree brix of the solution, the supersaturation (S) is calculated from Eq. (2):

$$S = \frac{^{\circ}Bx/(100 - ^{\circ}Bx)}{^{\circ}Bx_{\mathrm{sat}}/(100 - ^{\circ}Bx_{\mathrm{sat}})} \tag{2}$$

where $^{\circ}Bx_{\mathrm{sat}}$ is the degree brix of a saturated solution at the same temperature. Considering T to be the temperature of the solution in degree Celsius, $^{\circ}Bx_{\mathrm{sat}}$ is calculated by the following empirical expression [11]:

$$^{\circ}Bx_{\mathrm{sat}} = 64.447 + 8.22 \times 10^{-2}T + 1.66169 \times 10^{-3}T^2 - 1.558 \times 10^{-6}T^3 - 4.63 \times 10^{-8}T^4 \tag{3}$$

Temperature and consequently supersaturation is automatically controlled by two PID controllers in a cascade set-up, as represented in Fig. 6.

2.2. Process operation strategy

The overall process operation strategy was the same in all experiments. This strategy consisted of dividing the process into three phases: dissolution, crystallisation and stabilisation phases.

During the dissolution phase, an initial amount of sucrose and water is inserted in the crystalliser and the temperature is kept constant at 60 $^{\circ}$ C for 10–20 h. A long dissolution phase

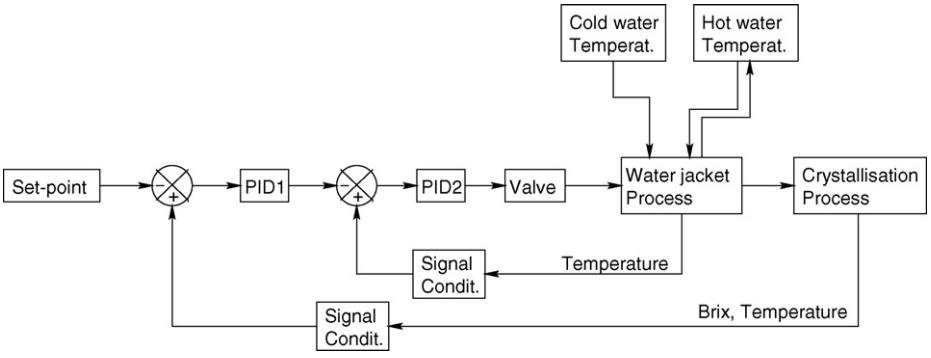

Fig. 6. Block diagram of the cascade control system.

ensures that all sucrose is diluted and any further nucleation will not result from eventual microscopic crystals that could otherwise still exist in the system.

At the end of the dissolution phase, the degree brix is adjusted to 72% by adding water to the system. The crystallisation is then started. The temperature decreases, making the supersaturation rise. When supersaturation exceeds 1.05 the system is seeded with 0.2 ml of a 50% ethanol/milled sugar mixture. After this, the supersaturation automatic control takes over and maintains supersaturation at 1.15 by lowering the temperature as sucrose passes to the solid phase.

The crystallisation phase lasts more than 24 h, allowing the degree brix to lower from 72 to 69%. When this value reaches 69%, the process is stopped by lowering the supersaturation setpoint to 1.01. At such a low supersaturation, the crystallisation kinetics are so slow the system may be considered at equilibrium for all practical purposes.

3. System model: balance equations

The model now presented simulates the evolution in time of sucrose concentration, crystal size distribution and agglomeration degree distribution. The temperature in the crystalliser is not simulated. Its value is acquired during the experiments and used in the simulator.

The extensive variables include the mass of sucrose in solution, mass of water, mass of crystals and number of crystals. These are normalised by the total mass of the system, making the simulator independent of its size.

3.1. Crystal number population balance

Let n_i be the number of crystals larger then L_i and smaller than L_{i+1}, per unit mass of the system. $\bar{L}_i$ is the mean value of L of the ith size interval and Δi its amplitude. Eq. (4) represents the relations between the variables. N_{disc} is the total number of size intervals and $r = \sqrt[3]{2}$ the geometric progression ratio:

$$L_i = r^{(i-1)}L_1, \qquad \bar{L}_i = \frac{r+1}{2}L_i,$$
$$\Delta L_i = (r-1)L_i, \quad i = 1 \rightarrow N_{\text{disc}} \tag{4}$$

The change rate of the total number of crystals in interval i, $(\mathrm{d}n_i/\mathrm{d}t)_{\text{total}}$, is the sum of the contributions of nucleation, $(\mathrm{d}n_i/\mathrm{d}t)_{\text{nuc}}$, growth, $(\mathrm{d}n_i/\mathrm{d}t)_{\text{growth}}$ and agglomeration $(\mathrm{d}n_i/\mathrm{d}t)_{\text{aggl}}$ given in Eq. (5):

$$\left(\frac{\mathrm{d}n_i}{\mathrm{d}t}\right)_{\text{total}} = \left(\frac{\mathrm{d}n_i}{\mathrm{d}t}\right)_{\text{nuc}} + \left(\frac{\mathrm{d}n_i}{\mathrm{d}t}\right)_{\text{growth}} + \left(\frac{\mathrm{d}n_i}{\mathrm{d}t}\right)_{\text{aggl}} \tag{5}$$

3.1.1. Nucleation

In the present model, it was considered that all new crystals produced by nucleation appear in the first discretisation size class according to the kinetic model introduced by Larson [12] and Bennet [13] and further adapted to sucrose batch crystallisation by Chorão and Feyo de Azevedo [11]. The contribution of the nucleation rate to the crystal number population balance is represented by the kinetic term B_0 in units of number of new nuclei per unit time and per unit mass in the system. This is calculated by Eq. (6):

$$\left(\frac{\mathrm{d}n_1}{\mathrm{d}t}\right)_{\text{nuc}} = B_0 \tag{6}$$

3.1.2. Growth

The discretisation of the growth model, employed in this work, was proposed by Chorão and Feyo de Azevedo [11]. This model also considers the growth rate dispersion phenomena. The growth rate expression is presented in Eq. (7):

$$\left(\frac{\mathrm{d}n_i}{\mathrm{d}t}\right)_{\text{growth}} = 3.5\frac{G}{L_i}\left(n_{i-1} - \frac{1}{r}n_i\right) + 3.2\frac{D_{\text{g}}}{L_i^2}\left(n_{i-1} - \frac{1}{r^2}n_i\right) \tag{7}$$

3.1.3. Agglomeration

The discretised agglomeration model used in this work was proposed by Hounslow et al. [10] and is presented in Eq. (8):

$$\left(\frac{\mathrm{d}n_i}{\mathrm{d}t}\right)_{\text{aggl}} = n_{i-1}\sum_{j=1}^{i-1}\left[2^{j-i+1}\beta_{i-1,j}n_j\right] + \frac{1}{2}\beta_{i-1,i-1}n_{i-1}^2 - n_i\sum_{j=1}^{i-1}\left[2^{j-i}\beta_{i,j}n_j\right] - n_i\sum_{j=i}^{N_{\text{disc}}}\left[\beta_{i,j}n_j\right] \tag{8}$$

This equation results from the sum of four distinct terms. The first two are positive terms and correspond to the birth of crystals in the given discretisation interval. The other two terms are negative and correspond to the death of crystals:

(1) birth in size class i by agglomeration of crystals from class $i-1$ with crystals from classes 1 to $i-2$;
(2) birth in size class i by agglomeration of crystals from class $i-1$;
(3) death in size class i by agglomeration of crystals from class i with crystals from classes 1 to $i-1$;
(4) death in size class i by agglomeration of crystals from class i with crystals from classes i to N_{disc};

In Eq. (8), β represents the kinetic term of the agglomeration kernel.

3.2. Agglomeration degree population balance

The development of a new image analysis technique, namely the measurement of the agglomeration degree [8], makes it possible to use this information for model development and validation. To the best of our knowledge, this is the first time that a model for simulating this property is presented. It is based on the technique employed to measure this variable and makes sense in this context.

The model derives from the following set of conditions:

(1) the agglomeration degree, quantified by the variable Ag, is a number that may take any value between 0 and 1;
(2) the agglomeration degree increases with the increase of the complexity of the crystal;
(3) all crystals with an agglomeration degree less than 0.25 are considered to be not agglomerated (simple crystals);
(4) at any time, the agglomeration degree of a discretisation size class is the average of the agglomeration degrees of all crystals with a size corresponding to this class;
(5) all crystals belonging to size class i are considered to have an agglomeration degree of Ag_i—the agglomeration degree of size class i;
(6) when a crystal grows from size class $i-1$ to class i, the agglomeration degree of size class i changes by introducing a new crystal with agglomeration degree Ag_{i-1};
(7) the agglomeration degree of a new crystal (Agn), resulting from the agglomeration of two original crystals is equal to the sum of the relative size weighted average of their agglomeration degrees with a term corresponding to this agglomeration event;
(8) when a new crystal is formed by agglomeration, the agglomeration degree of its size class changes with the introduction of a new crystal with agglomeration degree Agn.

Conditions 1–4 are a direct consequence of the image analysis technique previously developed by the authors [8] and the subsquent statistical treatment of the data. The discretised nature of the model establishes the conditions 5, 6 and 8.

The seventh condition may be divided into two distinct parts, each one corresponding to one of the two terms of the sum—the weighted average of the agglomeration degrees and the increase in the agglomeration degree due to the agglomeration event itself.

The first part results from the criteria established to build the four classes of the agglomeration tree [8]—simple, small, medium or high agglomeration. The resulting classification of an agglomeration between a large and a small crystal is practically independent of the agglomeration degree of the small crystal as the predominant shape is that of the larger crystal, no matter how agglomerated the two crystals may be.

The second part (viz. the second term of the sum) produces an increase in the agglomeration degree due to the agglomeration in course. The quantification of this increase must agree with the original classification tree and the equations derived to measure the agglomeration degree from image analysis data. The following qualitative observations may be derived. These shall be used in the development of the model equation:

- If two simple crystals of the same size agglomerate, the resulting crystal is classified as medium agglomerated (MA), that is with an agglomeration degree around 2/3;
- In order to produce a small agglomerated crystal (SA) from two simple crystals, one of the original crystals must be considerably smaller than the other. The agglomeration degree of an SA crystal should be close to 1/3;
- Very agglomerated crystals (VA) always result from agglomeration between crystals which were already classified as agglomerated. The agglomeration degree of a VA crystal is higher than 0.75;
- The resulting crystal of agglomeration between an SA crystal with a considerably smaller one should be classified as MA.

Eq. (9) defines the agglomeration degree of a new crystal ($\mathrm{Agn}_{i,j}$), born from the agglomeration of two original crystals belonging to size classes i and j, with agglomeration degrees Ag_i and Ag_j and sizes $\bar{L}_i$ and $\bar{L}_j$:

$$\mathrm{Agn}_{i,j} = \frac{\bar{L}_i^2\mathrm{Ag}_i + \bar{L}_j^2\mathrm{Ag}_j}{\bar{L}_i^2 + \bar{L}_j^2} + \frac{1}{\left|2(\bar{L}_i - \bar{L}j)/(\bar{L}_i + \bar{L}j)\right| + 1} \times \left(1 - \frac{\bar{L}_i^2\mathrm{Ag}_i + \bar{L}_j^2\mathrm{Ag}_j}{\bar{L}_i^2 + \bar{L}_j^2}\right)\frac{2}{3} \quad (9)$$

The first term of this equation corresponds to the calculation of the mean value of the original agglomeration degrees using an area weighted average. In the training stage of the image analysis technique [8], the technician visually classifies the agglomeration degree of the crystals based on a two-dimensional projection of their shape.

The second term of the sum is the product of three factors. The third one, 2/3, represents the agglomeration degree resulting from the agglomeration of two identically sized simple crystals.

The first factor accounts for the effect of the difference in size between the two original crystals. If they have the same size, this first factor is neutral as it takes the value of 1. Otherwise, it approaches 1/3 with the increase in the size difference of the original crystals, lowering the agglomeration degree of the new crystal.

The second factor lowers the increase in the agglomeration degree of the new crystal as the agglomeration degree of the original crystals increases. This factor assures that the agglomeration degree of the new crystal is never greater than 1.

The evolution in time of the agglomeration degree of each size class can now be developed simply by counting the number of crystals going in and out of a given size class and their respective agglomeration degree.

Let $\mathrm{Ag}_i(t_0)$ be the mean agglomeration degree of the crystals in size class i at instant t_0. At $t_0 + \Delta t$, the agglomeration degree $\mathrm{Ag}_i(t_0 + \Delta t)$ represents the average of the following terms:

- agglomeration degree of crystals in size class i, at instant t_0;
- agglomeration degree of crystals that enter this size class by growth or agglomeration during the time interval Δt;
- agglomeration degree of crystals that leave this size class also by growth or agglomeration, during the time interval Δt.

From a practical point of view, $\mathrm{Ag}_i(t_0 + \Delta t)$ is simply the quotient between the first-order moment of the agglomeration degree distribution in each size class (μ_{1,Ag_i}) and the zeroth order moment (μ_{0,Ag_i}), at time $t_0 + \Delta t$ (Eq. (10)):

$$\mathrm{Ag}_i(t_0 + \Delta t) = \frac{\mu_{1,\mathrm{Ag}_i}}{\mu_{0,\mathrm{Ag}_i}} \quad (10)$$

The zeroth order moment is simply calculated by adding the number of crystals of the size class at moment t_0 with the

respective crystal number variation between t_0 and $t_0 + \Delta t$ (Eq. (11)):

$$\mu_{0,\mathrm{Ag}_i}(t_0 + \Delta t) = n_i(t_0) + \int_{t_0}^{t_0+\Delta t} \left(\frac{\mathrm{d}n_i}{\mathrm{d}t}\right)_{\text{total}} \mathrm{d}t \tag{11}$$

In order to calculate the first-order moment, one must know how many crystals were in the size class, how many are going in or out of the interval and also the respective agglomeration degree of the crystals. This may be achieved through the discretised population balance used to model the population size balance.

Eqs. (7) and (8) are a sum of terms. The positive terms account for crystals going into size class i. These must be multiplied by the agglomeration degree of the size class they originated from. In the case of growth, this is Ag_{i-1} and, in the case of agglomeration between a crystal from size class m with a crystal from size class n, it is $\mathrm{Agn}_{m,n}$, calculated from Eq. (9).

The negative terms account for crystals leaving interval i. Considering condition 5 of this model, these crystal have an agglomeration degree of Ag_i. The first-order moment may then be calculated by Eq. (12):

$$\begin{aligned}
&\mu_{1,\mathrm{Ag}_i}(t_0 + \Delta t) \\
&= n_i(t_0)\mathrm{Ag}_i(t_0) + \int_{t_0}^{t_0+\Delta t} \left(3.5\frac{G}{L_i} + 3.2\frac{D_\mathrm{g}}{L_i^2}\right) n_{i-1}\mathrm{Ag}_{i-1}\,\mathrm{d}t \\
&- \int_{t_0}^{t_0+\Delta t} \left(3.5\frac{G}{rL_i} + 3.2\frac{D_\mathrm{g}}{r^2L_i^2}\right) n_i\mathrm{Ag}_i\,\mathrm{d}t \\
&+ \int_{t_0}^{t_0+\Delta t} n_{i-1}\sum_{j=1}^{i-1}\left[2^{j-i+1}\beta_{i-1,j}n_j\mathrm{Agn}_{i-1,j}\right]\,\mathrm{d}t \\
&+ \int_{t_0}^{t_0+\Delta t} \frac{1}{2}\beta_{i-1,i-1}n_{i-1}^2\mathrm{Agn}_{i-1,i-1}\,\mathrm{d}t \\
&- \int_{t_0}^{t_0+\Delta t} \mathrm{Ag}_i n_i\sum_{j=1}^{i-1}\left[2^{j-i}\beta_{i,j}n_j\right]\,\mathrm{d}t \\
&- \int_{t_0}^{t_0+\Delta t} \mathrm{Ag}_i n_i\sum_{j=i}^{N_\mathrm{disc}}\left[\beta_{i,j}n_j\right]\,\mathrm{d}t
\end{aligned} \tag{12}$$

The agglomeration degree time balance equation may be calculated from the derivative definition, presented in Eq. (13):

$$\left.\frac{\mathrm{d}\mathrm{Ag}_i}{\mathrm{d}t}\right|_{t_0} = \lim_{\Delta t\to 0}\frac{\mathrm{Ag}_i(t_0+\Delta t) - \mathrm{Ag}_i(t_0)}{\Delta t} \tag{13}$$

Combining Eqs. (10)–(12) and replacing $\mathrm{Ag}_i(t_0 + \Delta t)$ in Eq. (13), yields Eq. (14):

$$\frac{\mathrm{d}\mathrm{Ag}_i}{\mathrm{d}t} = \frac{\begin{array}{l}(3.5(G/L_i) + 3.2(D_\mathrm{g}/L_i^2))n_{i-1}\mathrm{Ag}_{i-1} - (3.5(G/rL_i) + 3.2(D_\mathrm{g}/r^2L_i^2))n_i\mathrm{Ag}_i + n_{i-1}\sum_{j=1}^{i-1}(2^{j-i+1}\beta_{i-1,j}n_j\mathrm{Agn}_{i-1,j}) \\ + (1/2)\beta_{i-1,i-1}n_{i-1}^2\mathrm{Agn}_{i-1,i-1} - \mathrm{Ag}_i n_i\sum_{j=1}^{i-1}(2^{j-i}\beta_{i,j}n_j) - \mathrm{Ag}_i n_i\sum_{j=i}^{N_\mathrm{disc}}(\beta_{i,j}n_j) - (\mathrm{d}n_i/\mathrm{d}t)\mathrm{Ag}_i\end{array}}{n_i} \tag{14}$$

The final form of the agglomeration degree balance equation is obtained by simplification of the previous equation where the $\mathrm{d}n_i/\mathrm{d}t$ term is expanded according to Eqs. (5), (7) and (8). The final result is presented in Eq. (15):

$$\frac{\mathrm{d}\mathrm{Ag}_i}{\mathrm{d}t} = \frac{(3.5(G/L_i) + 3.2(D_\mathrm{g}/L_i^2))n_{i-1}(\mathrm{Ag}_{i-1} - \mathrm{Ag}_i) + n_{i-1}\sum_{j=1}^{i-1}2^{j-i+1}\beta_{i-1,j}n_j(\mathrm{Agn}_{i-1,j} - \mathrm{Ag}_i) + (1/2)\beta_{i-1,i-1}n_{i-1}^2(\mathrm{Agn}_{i-1,i-1} - \mathrm{Ag}_i)}{n_i} \tag{15}$$

3.3. Mass balance

As the considered system is closed, all mass variables are normalised by the total suspension mass in the system. The water mass is always constant and sucrose may only transfer from the solution to the solid phase. Considering w_suc to be the mass of sucrose per unit mass of suspension and w_c the mass of crystals per unit mass of suspension, the mass balance may be represented by Eq. (16):

$$\frac{\mathrm{d}w_\mathrm{suc}}{\mathrm{d}t} = -\frac{\mathrm{d}w_\mathrm{c}}{\mathrm{d}t} = J_\mathrm{cris} \tag{16}$$

In this equation, J_cris represents the global crystallisation rate in units of sucrose mass, transferred from the solution to the crystalline phase, per unit time and per unit mass of suspension. Its value is calculated from Eq. (17), from the rate of change in the number of crystals due to growth and nucleation:

$$J_\mathrm{cris} = \rho_\mathrm{c}k_\mathrm{v}\sum_{i=1}^{N_\mathrm{disc}}\bar{L}_i^3\left[\left(\frac{\mathrm{d}n_i}{\mathrm{d}t}\right)_\mathrm{nuc} + \left(\frac{\mathrm{d}n_i}{\mathrm{d}t}\right)_\mathrm{growth}\right] \tag{17}$$

4. System model: kinetic equations

To complete the model, the growth, nucleation and agglomeration kinetics must be defined. The variables G, D_g, B_0 and β must be determined.

4.1. Growth rate

At temperatures greater than 50 °C, the growth rate of sucrose crystals is controlled by the diffusion step [14]. At lower temperatures, the integration step controls growth. In the experiments carried out for this work, the crystalliser operation temperatures varied between 20 and 40 °C. This way, it was considered that the integration step is always the limiting factor in the overall growth rate.

Sá et al. [15] determined, experimentally, the sucrose growth kinetics at 40 °C. The results obtained by these authors, revealed

Table 1
Results referring to the value of kg_2 in Eq. (18) [15]

$\bar{L} = 0.393$ mm, $kg_2 = 1.21 \pm 0.1$
$\bar{L} = 0.597$ mm, $kg_2 = 1.23 \pm 0.06$
$\bar{L} = 0.853$ mm, $kg_2 = 1.25 \pm 0.06$

a dependency not only on the sucrose concentration but also on the crystal size. Measuring the sucrose supersaturation as the difference between its value in the bulk solution and the equilibrium value at the same temperature (ΔC), the authors derived Eq. (18):

$$R_g = K_{R_g} \bar{L}^{kg_1} \Delta C^{kg_2} \tag{18}$$

The value of K_{R_g}, found by the authors was 6.84×10^{-3}, with ΔC expressed in units of sucrose mass per mass of water, the mean crystal size ($\bar{L}$) expressed in meters and R_g, the growth rate per unit surface area of crystals expressed in kilogram of sucrose per second and per square meter. The best value of kg_1 found was 0.54 while kg_2 revealed some dependency on crystal size as may be seen from Table 1.

These results were obtained from experiments carried out at 40 °C. As in the present work the temperature in the crystalliser oscillated between 20 and 40 °C, it is necessary to correct the value of K_{R_g} according to Eqs. (19) and (20). As for kg_1 and kg_2, the estimated values for 40 ° C shall be used:

$$R_g = \frac{1}{A}\frac{dm_c}{dt} = K_{g_0} e^{-E_g/RT}(c - c_{sat})^g \tag{19}$$

$$K_{R_g} = K'_{R_g} \exp\left(\frac{-E_g}{RT}\right) \tag{20}$$

VanHook [16] presents the following values of E_g for the temperature interval of the present work:

$T = 20\,°C \rightarrow E_g = 70.7$ kJ/mol,

$T = 30\,°C \rightarrow E_g = 67.4$ kJ/mol,

$T = 40\,°C \rightarrow E_g = 62.6$ kJ/mol

Replacing the value of K_{R_g} estimated by Sá et al. [15] and the value of E_g at 40 ° C presented, in Eq. (20), a theoretical value of $K'_{R_g} = 1.89 \times 10^8$ is determined.

In the model used in the present work, the growth rate is expressed in units of crystal length per unit time (G) through Eq. (21). In order to compare the experimental results obtained with the ones presented by Sá et al. [15] it is necessary to calculate the value of K_g from the literature value of K_{R_g}. This is achieved through Eq. (22)[17] and the values of the volume shape factor $k_v = 0.102$ and the surface shape factor $k_a = 1.33$. These shape factors were experimentally determined using the equivalent diameter of the crystal projected shape area, obtained through image analysis. The resulting value of K_g, obtained from the results of Sá et al. [15] is then $K_g = 5.2 \times 10^5$, with G expressed in units of meters per second:

$$G = K_g \exp\left(-\frac{E_g}{RT}\right) \bar{L}^{kg_1} \Delta C^{kg_2} \tag{21}$$

$$R_g = \frac{1}{A}\frac{dm_c}{dt} = \frac{1}{k_a L^2}\frac{d(\rho_c k_v L^3)}{dt} = \frac{3\rho_c k_v}{k_a} G \tag{22}$$

The growth rate dispersion is modelled according to Randolph and White [18], for pure solutions. The growth rate dispersion kinetics (D_g) is calculated from Eq. (23):

$$D_g = 5 \times 10^{-5} G \text{ m}^2/\text{s} \tag{23}$$

4.2. Nucleation kinetics

As the system was operated at relatively low supersaturation and seeds were introduced in the system, only secondary nucleation is expected.

The kinetic model used to simulate the nucleation kinetics is the same used by Chorão and Feyo de Azevedo [11] in the simulation of an industrial batch sugar crystalliser. It is an empirical model deduced from the work of Sowul and Epstein [19], Larson [12] and Bennet [13]. It predicts the birth number rate of new crystals per unit mass in the system (B_0) from the values of the growth rate, and the ratio of crystal mass per unit volume of the system (Eq. (24)):

$$B_0 = \frac{K_b}{\rho_m} G^{b_1} \left(\frac{\rho_m}{\rho_c}\frac{w_c}{k_v}\right)^{b_2} \tag{24}$$

The values predicted by Chorão and Feyo de Azevedo [11] for the constants K_b, b_1 and b_2 and for the industrial crystalliser were, respectively, 2.894×10^{12}, 0.51 and 0.53 which, in the absence of better estimates, were used in this work.

4.3. The agglomeration kernel

In the model being presented, the agglomeration rate $\beta(L_i, L_j)$ represents the probability of a crystal from size class L_i agglomerating with a crystal from size class L_j. According to Chorão and Feyo de Azevedo [11], based on the works of Moller [20], David et al. [21] and Marchal et al. [22], this probability is proportional to the crystal surface area, the growth rate, the mass of crystals in suspension and inversely proportional to the mass of the crystal. Therefore, it is a function of the crystal size.

According to Kuijvenhoven et al. [23], Austmeyer [24], Kamoda and Yamane [25], Ziegler [26] and Moller [20], there is a minimum and a maximum size beyond which there is no agglomeration and a critical size for which the agglomeration probability is highest. However such values are far from being in agreement. In the present work, just as in the work of Chorão and Feyo de Azevedo [11], the minimum size was considered to be 10 μm, the maximum 250 μm and the critical size (L_{crit}) 100 μm.

Eq. (25) was then used to quantify the agglomeration rate:

$$\beta_{i,j} = K_{ag} \frac{(L_{crit} L_i L_j)^2}{(1/2L_{crit}^3 + L_i^3)(1/2L_{crit}^3 + L_j^3)} G \left(\frac{w_c}{k_v}\frac{\rho_m}{\rho_c}\right) \tag{25}$$

Table 2
Summary of the mass balance equations

Eqs. (16) and (17): $\frac{dw_{suc}}{dt} = -\rho_c k_v \left[\frac{dn_1}{dt} + \sum_{i=2}^{N_{disc}} \left(\frac{dn_i}{dt}\right)_{growth}\right]$

5. Simulation

The model presented was used to predict the sugar contents, crystal size distribution and agglomeration degree distribution in the laboratory crystalliser. A Fortran77 subroutine was developed to apply a Runge-Kutta 4th/5th order integration subroutine previously developed and extensively tested. As the goal of this work was not to test the crystallisation thermodynamics, the temperature in the crystalliser was not simulated. The values acquired during the experimental work were used in the simulator. A summary of the equations is presented in Tables 2–7.

Although the crystal size measuring device (a Coulter LS9000 laser granulometer) has a sensibility to detect particles as small as 0.4 μm, no crystals were detected below 0.9 μm. Based on this result and previous experience, 0.9 μm was chosen as the minimum crystal size for size discretisation purposes. All crystals born by nucleation appear in the first size class. The number of discretisation size classes (N_{disc}) is 39. The simulation starts the moment the seeds are introduced in the system and ends when the supersaturation reaches its final value (1.01). The initial values of the mass variables are presented in Table 8.

The initial value of the variables n_i is the number of crystals introduced through seeding, calculated from the seeds CSD and their mass per unit total mass in the crystalliser (w_{seed}). Eq. (26) was used to calculate these values from the volume cumulative CSD ($V_{seed}(L)$) presented in Fig. 7. As the seeds are produced by abrasion, their shape is expected to be approximately spherical and thus the value of k_v used in this equation is $\pi/6$:

$$n_i = w_{seed} \frac{(V_{seed}(L_{i+1}) - V_{seed}(L_i))/100}{\rho_c k_v \bar{L}_i^3} \quad (26)$$

The seeds are neither simple crystals nor agglomerates. They are fragments of crystals without any characteristic shape. Nevertheless, as they grow, they are expected to tend to assume the shape of simple crystals. This way, the assumed initial value of the agglomeration degree is 0 ($Ag_i(t=0) = 0$).

Table 3
Summary of the CSD balance equations

(Eqs. (5)–(7)): $\frac{dn_1}{dt} = B_0 - 3.5 n_1 \frac{G}{rL_1} - 3.2 n_1 \frac{D_g}{r^2 L_1^2}$
(Eq. (7)): $\left(\frac{dn_{N_{disc}}}{dt}\right)_{growth} = 3.5 n_{N_{disc}-1} \frac{G}{L_{N_{disc}}} + 3.2 n_{N_{disc}-1} \frac{D_g}{L_{N_{disc}}^2}$
(Eq. (7)): $\left(\frac{dn_i}{dt}\right)_{growth} = 3.5 \frac{G}{L_i}\left(n_{i-1} - \frac{1}{r} n_i\right) + 3.2 \frac{D_g}{L_i^2}\left(n_{i-1} - \frac{1}{r^2} n_i\right), \quad i = 2, N_{disc} - 1$
$\left(\frac{dn_i}{dt}\right)_{aggl} = n_{i-1} \sum_{j=1}^{i-1}\left[2^{j-i+1}\beta_{i-1,j} n_j\right] + \frac{1}{2}\beta_{i-1,i-1} n_{i-1}^2 - n_i \sum_{j=1}^{i-1}\left[2^{j-i}\beta_{i,j} n_j\right] - n_i \sum_{j=i}^{N_{disc}}\left[\beta_{i,j} n_j\right]$
(Eq. (5)): $\left(\frac{dn_i}{dt}\right)_{total} = \left(\frac{dn_i}{dt}\right)_{growth} + \left(\frac{dn_i}{dt}\right)_{aggl}, \quad i = 2, N_{disc}$

Table 4
Summary of the agglomeration degree balance equations

$\frac{dAg_1}{dt} = 0$
(Eq. (15)): $\frac{dAg_i}{dt} = \frac{\begin{array}{c}(3.5(G/L_i) + 3.2(D_g/L_i^2)) n_{i-1} Ag_{i-1} - (3.5(G/rL_i) + 3.2(D_g/r^2 L_i^2)) n_i Ag_i + n_{i-1} \sum_{j=1}^{i-1} (2^{j-i+1} \beta_{i-1,j} n_j Agn_{i-1,j}) \\ + (1/2)\beta_{i-1,i-1} n_{i-1}^2 Agn_{i-1,i-1} - Ag_i n_i \sum_{j=1}^{i-1} (2^{j-i} \beta_{i,j} n_j) - Ag_i n_i \sum_{j=i}^{N_{disc}} (\beta_{i,j} n_j) - (dn_i/dt) Ag_i\end{array}}{n_i}, \quad i = 2, N_{disc}$

Table 5
Summary of the kinetic equations

Growth kinetics
(Eq. (21)): $G = K_g \exp\left(\frac{-67{,}400}{8.314(T_m + 273.15)}\right) \Delta C^{86.58} \bar{L} + 1.1768 \bar{L}^{0.54}$
(Eq. (23)): $D_g = 5 \times 10^{-5} G$
Nucleation kinetics
(Eq. (24)): $B_0 = \frac{K_b}{\rho_m} G^{0.5} \left(\frac{w_c \rho_m}{\rho_c k_v}\right)^{0.5}$
Agglomeration kinetics
(Eq. (25)): $\beta_{i,j} = K_{ag} \frac{(L_{crit} L_i L_j)^2}{(0.5 L_{crit}^3 + L_i^3)(0.5 L_{crit}^3 + L_j^3)} G \frac{w_c \rho_m}{\rho_c k_v}, \quad \text{if } 10^{-5} < L_i < 5 \times 10^{-2} \wedge 10^{-5} < L_j < 5 \times 10^{-2}$
(Eq. (9)): $Agn_{i,j} = \frac{\bar{L}_i^2 Ag_i + \bar{L}_j^2 Ag_j}{\bar{L}_i^2 + \bar{L}_j^2} + \frac{1}{\lvert(\bar{L}_i - \bar{L}_j)/[(\bar{L}_i + \bar{L}_j)/2]\rvert + 1}\left(1 - \frac{\bar{L}_i^2 Ag_i + \bar{L}_j^2 Ag_j}{\bar{L}_i^2 + \bar{L}_j^2}\right)\frac{2}{3}$

Table 6
Summary of the physical properties [11]

$\rho_c = 1580\,\text{kg/m}^3$
$\rho_s = \left(1000 + {}^\circ Bx_s \frac{200+{}^\circ Bx_s}{54}\right)\left(1 - 0.036\frac{T(K)-20}{160-T(K)}\right)\,\text{kg/m}^3$
$\rho_m = \frac{\rho_c \rho_s}{\rho_c - w_c(\rho_c-\rho_s)}$
${}^\circ Bx_{sat} = 64.447 + 8.222\times10^{-2}T_m + 1.66169\times10^{-3}T_m^2 - 1.558\times10^{-6}T_m^3 - 4.63\times10^{-8}T_m^4$

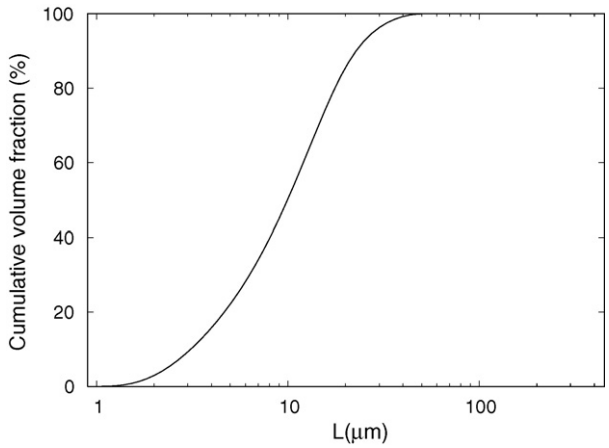

Fig. 7. Volume fraction CSD of the seeds.

6. Parameter estimation and model validation

The simulator, together with a set of two experimental results obtained in the experimental set-up presented in the first part of this work, was used to validate the model and estimate the nucleation, growth and agglomeration kinetic parameters.

The non-linear optimisation was carried out through a least squares algorithm developed by Meyer and Roth [27] and implemented in a Fortran77 subroutine.

The objective function (Obj), presented in Eq. (27), uses the experimental and simulated results of the sugar concentration (degree brix) profile, the final CSD and the final agglomeration

Table 7
Summary of the auxiliary equations

Referring to the suspension
$w_c = 1 - (w_{suc} + w_w)$
${}^\circ Bx_s = 100\frac{w_{suc}}{w_{suc}+w_w}$
$S = \frac{{}^\circ Bx_s/(100-{}^\circ Bx_s)}{{}^\circ Bx_{sat}(100-{}^\circ Bx_{sat})}$
$\Delta C = (S-1)\frac{{}^\circ Bx_{sat}}{100-{}^\circ Bx_{sat}}$
Referring to the CSD discretisation
$r = \sqrt[3]{2}$
$k_v = 0.102$
$L_{crit} = 150\times10^{-6}\,\text{m}$
$N_{disc} = 39$
$L_1 = 0.9\times10^{-6}\,\text{m}$
$L_i = rL_{i-1}, \quad i = 2 \rightarrow N_{disc}$
$\bar{L}_i = \frac{r+1}{2}L_i, \quad i = 1 \rightarrow N_{disc}$

Table 8
Summary of the initial values of the mass variables

$w_{seed} = 4.56\times10^{-6}$
$w_{c,t=0} = w_{seed}$
$w_w = (1-w_{seed})\left(1 - \frac{{}^\circ Bx_{t=0}}{100}\right)$
$w_{suc,t=0} = 1 - w_w - w_{seed}$

degree distribution:

$$\text{Obj} = \frac{1}{N_{exp}}\sum_{i=1}^{N_{exp}}\left(\frac{{}^\circ Bx_{exp\,i} - {}^\circ Bx_{sim\,i}}{70}\right)^2 + \frac{1}{N_{disc}}\sum_{j=1}^{N_{disc}}\left(\frac{n_{exp\,j} - n_{sim\,j}}{0.5}\right)^2 + \frac{1}{N_{disc}}\sum_{k=1}^{N_{disc}}\left(\frac{\text{Ag}_{exp\,k} - \text{Ag}_{sim\,k}}{50}\right)^2 \quad (27)$$

The model contains several kinetic parameters, natural candidates for optimisation variables. If the number of optimisation parameters is high, the model validation looses meaning. As the goal of the present work is the evaluation of the model, only the three proportionality constants (K_g, K_b and K_{ag}) were optimised. Instead of using both sets of experimental data to calculate one single set of kinetic parameters, a set was calculated for each set of experimental data. The quality of the model is then judged by the differences in the parameter values. Table 9 presents the optimised value of these variables for each of the experimental results considered in the present work.

The growth rate presented by Sá et al. [15] resulted in a value of $K_g = 5.2\times10^5$. This value is roughly half of the one obtained in the experimental runs *S* _1.15_A and *S* _1.15_B. This can be explained by the differences in the operating conditions.

7. Results

With the optimised values presented in Table 9, it is possible to compare the accuracy of the model. Figs. 8 and 9 present these simulated and experimental results.

Table 9
Optimised value of the kinetic parameters

Refer.	K_g	K_b	K_{ag}	Obj
S _1.15_A	1.18×10^6	6.02×10^9	1.14×10^{-1}	1.35×10^{-3}
S _1.15_B	1.09×10^6	8.84×10^9	1.36×10^{-1}	1.42×10^{-3}

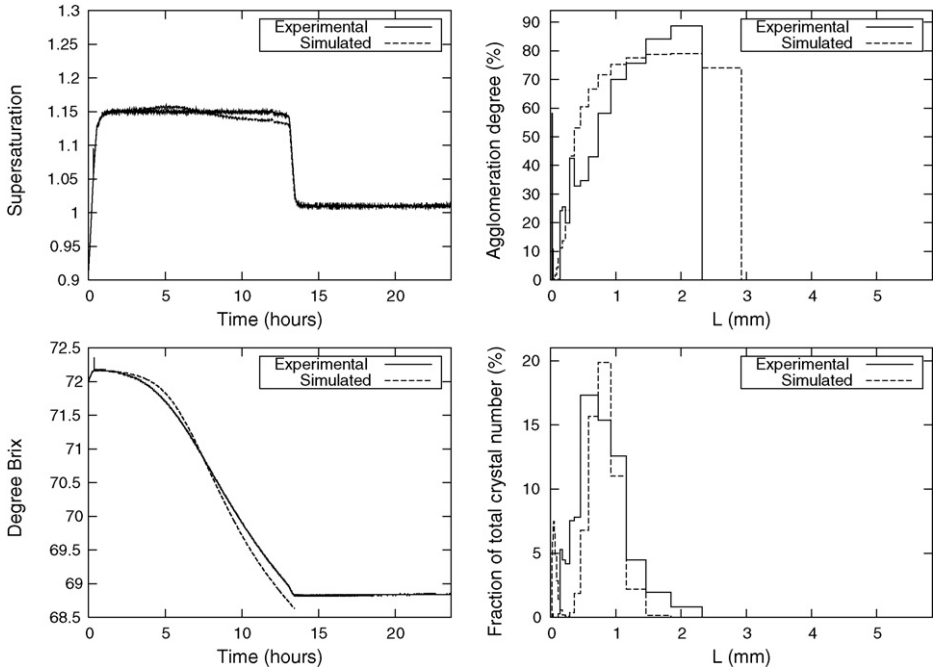

Fig. 8. Experimental and simulated results from experiment *S* _1.15_A.

This work presents, for the first time, an attempt to simulate the agglomeration degree distribution. It may be observed, from the figures, that the model tends to predict a higher agglomeration degree for the smaller crystals and a lower agglomeration degree for the larger ones. Also, the crystal size distribution model tends to predict smaller crystals than the ones observed by the image analysis technique. These two observations are probably related and may be due to two different reasons. The most obvious reason would be the agglomeration model failing to predict a higher agglomeration rate for bigger crystals. However, considering the experimental procedure previously described, it may happen that the crystals agglomerate during the filtration and drying phases which would result in the production of big, very aggregated crystals.

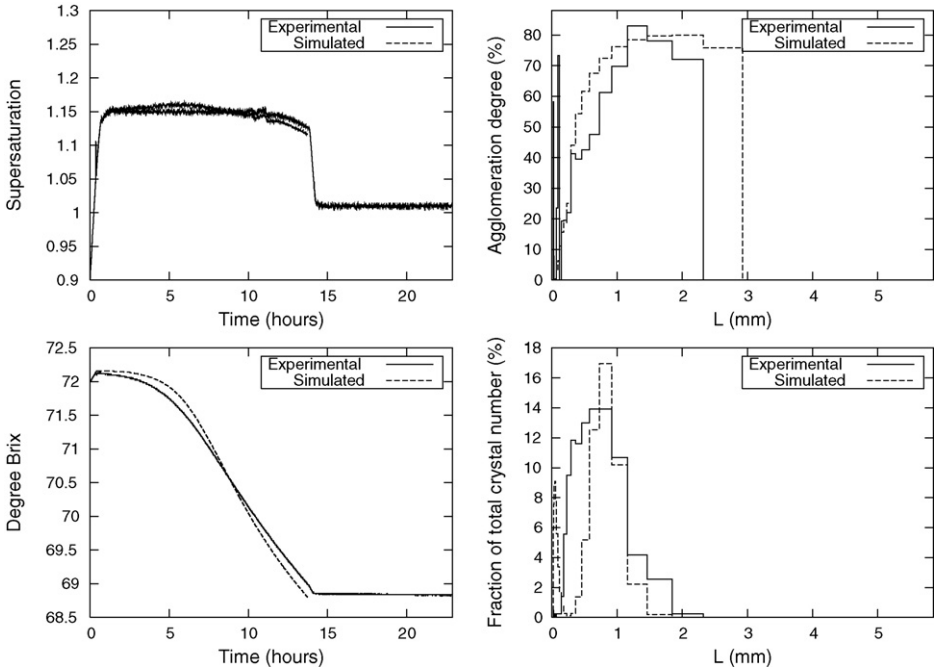

Fig. 9. Experimental and simulated results from experiment *S* _1.15_B.

8. Conclusion

The sugar crystallisation experimental facility provides reliable results. A model for predicting the agglomeration degree distribution of a population of sucrose crystals was developed and validated. This, together with the image analysis technique presented by Faria et al. [8], is an essential tool in the study of the agglomeration kinetics. A reliable experimental facility is mandatory when the final goal is the study of agglomeration mechanisms and kinetics.

Until now, agglomeration was only accounted for by its effect on the distribution of crystal sizes. It was necessary to have a priory knowledge of the growth rate, growth rate dispersion and nucleation kinetics to distinguish the agglomeration contribution to the shape of the crystal size distribution. The introduction of an independent and direct measurement of the agglomeration phenomenon allows a quantification of this phenomenon and consequently its effect on the crystal size distribution.

In order to improve the model presented, it is essential to follow the evolution of crystal properties as the experiments are carried out and not only the final result. It is known that crystal size and many other unaccounted for crystal properties have a strong effect on the agglomeration phenomena. During a batch crystallisation, the agglomeration kinetics should pass by drastically different values. Only if those values are measured as the experiment is conducted it will be possible to understand the mechanisms which will lead to the final agglomeration degree distribution.

The model here presented produced simulated results that predict the behaviour of the system with a precision similar to the spread of the experimental results between runs conducted under the same operating conditions. This was achieved through the estimation of only 3 kinetic parameters out of 11 natural candidates. The values considered for the other eight parameters were estimated by different authors in experimental conditions not always similar to the ones applied in this work. However, it is pointless to put in a big effort in model development and parameter estimation if this is not followed by an increase in the quality and quantity of experimental data available for model validation. The inclusion of a new independent measured variable in the model (the agglomeration degree) is a major step towards the broadening of the information contents used in model development.

Acknowledgements

This work was partially developed in the laboratories of the Research Unit Institute for Systems and Robotics "Instituto de Sistemas e Robótica-Porto", Portugal, and the "Laboratoire des Sciences du Génie Chimique", Nancy, France. It was partially financed by the "Ambassade de France", and by the Portuguese Foundation for Science and Technology "FCT-Fundação da Ciência e Tecnologia".

Appendix A. Nomenclature

A	surface area [L^2]
Ag_x	agglomeration degree of crystal x or size class x
$Agn_{x,y}$	agglomeration degree of a new crystal formed by agglomeration of a crystal x and a crystal y
b_1, b_2	parameter of the nucleation kinetics
B	birth rate of new crystals [T^{-1}]
B_0	nucleation rate [T^{-1}]
$^\circ Bx$	degree brix: mass percentage of dissolved solids (sucrose in this work)
c	mole concentration [NL^{-3}]
C	sucrose concentration (sucrose mass per water mass)
D	crystal "death" rate by agglomeration [T^{-1}]
D_g	linear growth rate dispersion [L^2T^{-1}]
E_G	crystal growth activation energy [$ML^2T^{-2}N^{-1}$]
G	linear crystal growth rate [LT^{-1}]
k_a	crystal surface shape factor
k_b	parameter of the nucleation kinetics equation
k_{g_1}, k_{g_2}	parameter of the linear growth rate kinetics equation
k_v	crystal volume shape factor
K_{ag}	parameter of the agglomeration kinetics equation
K_g	parameter of the linear growth rate kinetics equation
K_{R_g}	parameter of the mass growth rate kinetics equation
L	crystal linear size [L]
m	mass [M]
n_i	number of crystals in discretisation interval i, per unit mass of suspension [M^{-1}]
N	population density function in number[L^{-1}]
N_{disc}	number of crystal size discretisation intervals
N_{exp}	number of experimental points
N_i	number of crystals in the discretisation interval i
R_G	mass growth rate kinetics per unit surface area of crystals [$ML^{-2}T^{-1}$]
S	supersaturation
t	time [T]
T	temperature [Θ]
V	volume [L^3]
w	relative mass (mass per unit mass of suspension)

Greek characters

$\beta(x, y)$	probability of x size crystals agglomerating with y size crystals
μ_k	moment of order k of a statistics distribution function
ρ	specific gravity [ML^{-3}]

Indices and exponents

c	referring to crystals
exp	experimental values
m	referring to the masscuite
par	referring to the parameters
s	referring to the solution
sat	referring to the saturated solution
seed	referring to the seed crystals
sim	simulated value
suc	referring to sucrose

T total
w referring to water

Operators
ΔP finite variation of property P
$\bar{P}$ average value of property P

References

[1] Z. Bubník, P. Kadlec, Sucrose crystal shape factors, Zuckerind 117 (5) (1992) 345–350.
[2] P. Devillers, C. Cornet, Influence du raffinose sur la crystallisation du saccharose, in: Proceedings of the 14th Ass. CITS, Bruxelles, 1991.
[3] F. Kelly, The morphology of sucrose crystals, Sugar Technol. Rev. 3 (1982) 275–309.
[4] M. Saska, Calculated form of the sucrose crystal, Int. Sugar J. 85 (1017) (1983) 259–261.
[5] M. Saska, J.A. Polack, Effects of dextran on sucrose crystal shape, in: Proceedings of the 1982 Sugar Processing Research Conference, Louisiana, USA, 1992.
[6] D.N. Sutherland, Dextran and crystal elongation, Int. Sugar J. (1968) 355–358.
[7] D.N. Sutherland, N. Paton, Dextran and crystal elongation: further experiments, Int. Sugar J. (1969) 131–135.
[8] N. Faria, M.N. Pons, H. Vivier, S. Feyo de Azevedo, F.A. Rocha, H. Vivier, Quantifying the morphology of sucrose crystals by image analysis, Powder Technol. 133 (2003) 54–67.
[9] A.D. Randolph, M.A. Larson, Theory of Particulate Processes, Academic Press, 1971.
[10] M. Hounslow, R. Ryall, V. Marshall, A discretized population balance for nucleation, growth and aggregation, AIChE J. 34 (11) (1988) 1821–1832.
[11] J. Chorão, S. Feyo de Azevedo, A discretized population balance approach for the modelling of industrial sucrose crystallisation, in: Proceedings of the 13th Symposium on Industrial Crystallisation, Toulouse, France, 1996, pp. 719–725.
[12] M.A. Larson, Advances in the characterization of crystal nucleation, AIChE Symp. Ser. 80 (240) (1984) 39–44.
[13] R. Bennet, Advances in industrial crystallization techniques, Chem. Eng. Prog. (1984) 89–95.
[14] B. Smythe, Sucrose crystal growth, Sugar Technol. Rev. 1 (1971) 191–231.
[15] S. Sá, L. Guimaraes, F. Rocha, L. Bento, Growth and dissolution kinetics of sucrose crystals, in: Proceedings of the 13th Symposium on Ind. Cryst., vol. 1, Toulouse, 1996, pp. 385–390.
[16] A. VanHook, Growth of sucrose crystals—a review, in: Sugar Technology Reviews, Elsevier Scientific Publishing Company, 1981, pp. 41–79.
[17] J.W. Mullin, Crystallization, third ed., Butterworth Heinemann, 1993.
[18] A. Randolph, E. White, Modelling size dispersion in the prediction of crystal size distribution, Chem. Eng. Sci. 32 (1977) 1067–1076.
[19] L. Sowul, M. Epstein, Crystallization kinetics of sucrose in a cmsmpr evaporative crystallizer, Ind. Eng. Chem. Proc. Des. Dev. 20 (1981) 197–203.
[20] C. Moller, Sugar boiling theory and practice, Int. Sugar J. 85 (1983) 163–165.
[21] R. David, P. Marchal, J. Klein, J. Villermaux, Crystallization and precipitation engineering. iii. A discrete formulation of the agglomeration rate of crystals in a crystallization process, Chem. Eng. Sci. 46 (1991) 205–213.
[22] P. Marchal, B. Marcant, R. David, J.-P. Klein, The modelling of agglomeration in industrial crystallization from solution, in: AIChE Meeting, Los Angeles, 1991.
[23] L.J. Kuijvenhoven, L.M. De Pree, E.J. De Jong, Conglomerate formation in sugar crystallization. Part i. Effect of process conditions, Int. Sugar J. 85 (1015) (1983) 201–207.
[24] K. Austmeyer, Analysis of sugar boiling and its technical consequences. Part i. Supersaturation, crystal growth and the footing process, Int. Sugar J. 88 (1986) 3–7.
[25] M. Kamoda, T. Yamane, On the formation of conglomerates of sugar crystals, Proc. Res. Soc. Jpn. Sugar Ref. Tech. 8 (1959) 123–130.
[26] J. Ziegler, Sugar Boiling, Some Facts and Some Fancies, The Sugar Journal (1974) 56–84.
[27] R.R. Meyer, P.M. Roth, Modified damped least squares: an algorithm for non linear estimation, J. Inst. Math. Appl. 9 (1972) 218.